Research Article

Received: 29 November 2014 Revised: 30 January 2015 Accepted article published: 14 February 2015 Published online in Wiley Online Library: 6 March 2015

(wileyonlinelibrary.com) DOI 10.1002/pi.4894

Small and large scale segmental motion in polymers: estimating cooperativity length by ordinary relaxation experiments

Marco Pieruccini,[a*] Andrea Alessandrini,[a,b] Simone Sturniolo,[c,d] Maurizio Corti[d] and Attilio Rigamonti[d]

Abstract

We derive a suitable expression for estimating the size of the cooperatively rearranging regions (CRRs) in supercooled polymer melts by fitting data worked out by ordinary relaxation experiments carried out in isothermal conditions. As an example, the average CRR size in poly(*n*-butyl methacrylate) in proximity to the glass transition temperature is derived from a stress relaxation experiment performed by means of an atomic force microscopy setup. Good agreement is found with results in the literature derived from measurements of temperature fluctuations (the so-called Donth method). The temperature dependence of the CRR size is explored for poly(butadiene); in this case the segmental relaxation function is derived through a novel method for the analysis of the efficiency with which free induction decay echoes are refocused in ^{1}H NMR experiments. It is found that the CRR size increases upon cooling. The results derived from the analysis of the NMR data are found to be in satisfactory agreement with those worked out from broadband dielectric spectroscopy data in the literature.

Keywords: statistical mechanics; segmental relaxation; cooperativity; atomic force microscopy; nuclear magnetic resonance; dielectric spectroscopy

INTRODUCTION

Many properties of polymer based materials are related to segmental relaxations (also referred to as the α-process). For example, mechanical performances under different conditions, or the ability to support ion diffusion, depend on the dynamical features of these motions. The presence of configurational constraints such as crosslinks or chain pinnings to crystal surfaces, as well as the depletion of these constraints (e.g. when weakly interacting low molecular weight components are dispersed in the system), may have an influence in this respect, in particular with regard to the calorimetric glass transition temperature T_g. The cooperative nature of segmental motions and the characteristic length associated with them reflect these peculiarities; it may thus be important to estimate this length when customary methods for the analysis of these materials are used.

The basic idea of cooperative motion was given by Adam and Gibbs[1] some decades ago through the introduction of the concept of cooperatively rearranging region (CRR). Later, significant and fruitful advancements have been made by Donth[2] with the aim of elucidating the mechanisms underlying the phenomenon of the glass transition. One of his most popular results concerns the estimate of the characteristic cooperativity length close to T_g by the direct probing of temperature fluctuations in the CRRs.[3]

Donth's approach has been used to estimate the CRR size and its temperature dependence, from the combined analysis of scanning temperature heat spectroscopy and isothermal dielectric spectroscopy.[4] It was found that the CRR size increases on approaching T_g from above, consistent with the ideas put forward by Adam and Gibbs.

The aim of this contribution is to show how the CRR size can be estimated also by a different analysis of the loss component of the relaxation patterns, resolved in either time or frequency at constant temperature. Broadband dielectric spectra or stress data, for instance, represent cases where the application of this method is particularly suited, since they are usually recorded in isothermal conditions.

After a short outline of the theory at the basis of the method, the analysis of a stress relaxation experiment on poly(*n*-butyl methacrylate) (PnBMA) is carried out as an example. We perform these measurements by means of an AFM setup. In fact, AFM studies exploiting the force spectroscopy capability of this technique are becoming very popular in the study of polymeric materials.[5,6] Moreover, an increasing amount of work concentrates on the time or frequency domain of force spectroscopy in order to measure relaxation properties of samples.[7] A great advantage of AFM for this kind of experiment lies also in its possibility of mapping the

* *Correspondence to: Marco Pieruccini, CNR, Istituto Nanoscienze, v. Campi 213/A, 41125 Modena, Italy. E-mail: marco.pieruccini@nano.cnr.it*

a *CNR, Istituto Nanoscienze, v. Campi 213/A, 41125 Modena, Italy*

b *Dipartimento di Fisica Informatica e Matematica, Università di Modena e Reggio Emilia, v. Campi 213/A, 41125 Modena, Italy*

c *Rutherford Appleton Laboratory, Department of Computer Science, Chilton OX11 0QX, Oxfordshire, UK*

d *Dipartimento di Fisica, Università di Pavia, v. Bassi 6, 27100 Pavia, Italy*

lateral mechanical heterogeneity of a sample down to nanometre scale resolution. The results obtained by this technique will be shown to compare very well with independent measurements on PnBMA analysed following Donth's approach. Estimates of the cooperativity length from the isothermal mechanical response of semicrystalline poly(ethylene terephthalate) (PET) performed with the present scheme have already been shown[8] to be consistent with the results reported by Hamonic *et al.*[4]; this further supports the proposed approach. Finally, after a novel method for the analysis of ^{1}H NMR data is outlined, the temperature dependence of the CRR size in poly(butadiene) (PB) is estimated and a comparison is made with the results worked out from broadband dielectric measurements. Also in this case the agreement is good.

COOPERATIVE MOTION: OUTLINE OF THE THEORY

Configurational rearrangement in an undercooled polymer melt is assumed to take place in two consecutive steps. Let us consider initially a relatively small number of contiguous monomers moving about within a limited region of the configurational space. Then, after a suitable energy fluctuation, this group reaches an activated (mobility) state from which a subsequent larger scale rearrangement, involving a larger number of monomers, may occur. We refer to this 'fine structure' of the cooperative process as *small scale* and *large scale* cooperativities.

The description of the rearrangement statistics of an ensemble of such small sets of monomers has been the subject of a previous paper.[9] The main issues are that (i) all these small scale rearranging sets are formed by the same average number z of monomers, (ii) the energy threshold ζ (per monomer) for a rearrangement depends on the actual configuration of the z monomers and (iii) the average rearrangement chemical potential $\overline{\Delta\mu}$ of the mobile component of the whole system (i.e. all of the activated monomers, irrespective of the energy threshold they jumped above) is stationary. Under these conditions it is possible to derive the distribution $p(\zeta)$ for the number of monomers whose energy had to grow larger than ζ to reach the mobility state at temperature T. It is found that

$$p(\zeta) \approx e^{-\left[w(\zeta)\langle E\rangle_\zeta + \lambda\Delta\mu(\zeta)\right]/k_B T} \tag{1}$$

where $w(\zeta)$ is the probability that a monomer reaches the mobility state after gaining an energy $E \geq \zeta$, $\langle E\rangle_\zeta$ is the average energy of the states with $E \geq \zeta$ calculated accounting for their multiplicity, $k_B T$ is the thermal energy,

$$\Delta\mu(\zeta) \equiv -k_B T \ln w \tag{2}$$

and λ is a Lagrange multiplier associated with the condition

$$\overline{\Delta\mu} \equiv \int_0^\infty d\zeta p(\zeta)\Delta\mu(\zeta) = \text{const.} \tag{3}$$

The probability w is expressed in terms of the function

$$Z_{\zeta,n} \equiv \int_\zeta^\infty d\varepsilon\, \varepsilon^n e^{-\varepsilon/k_B T} \tag{4}$$

as

$$w = \frac{Z_{\zeta,n}}{Z_{0,n}} \tag{5}$$

with n an adjustable exponent that, upon data fitting, is always found to be a non-decreasing function of z.

After a set of z monomers has reached the activated state, it delivers back to the heat bath the energy $z\zeta$ just absorbed. If

$$w(\zeta) < e^{-s_c/k_B} \tag{6}$$

with s_c the configurational entropy, then this energy transfer occurs through the configurational degrees of freedom; otherwise the energy is forced to find other paths to regress. The above condition (Eqn (6)) states that the probability that a monomer is in the activated state is less than the probability of a configurational, low energy state.

The configurational entropy s_c can be expressed in terms of the specific heat step Δc_p at T_g and of the Kauzmann temperature T_K as

$$s_c = \Delta c_p \ln\left(\frac{T}{T_K}\right) \tag{7}$$

so the total number of rearranging monomers is

$$N_\alpha = z\left(1 + \frac{\kappa\overline{\zeta}}{Ts_c}\right) \tag{8}$$

where

$$\kappa = \left[\int_0^\infty d\zeta\, p\right]^{-1} \int_{\zeta_0}^\infty d\zeta\, p$$

is the fraction of small scale regions for which Eqn (6) is verified (ζ_0 being the value of ζ for which the equality holds in that equation) and

$$\overline{\zeta} = \left[\int_{\zeta_0}^\infty d\zeta\, p\right]^{-1} \int_{\zeta_0}^\infty d\zeta\, \zeta\, p$$

is the average energy associated with each of its monomers.

EXPERIMENTAL

Materials

PnBMA with average molecular weight 337 000 g mol^{-1} was purchased from Sigma-Aldrich, St. Louis, MO, USA. Samples of about 1 mm thickness were obtained from a saturated solution in toluene (150 mg mL^{-1}) after evaporation at a temperature of 313 K under vacuum for 1 week. According to the literature, the nominal glass transition temperature T_g is *ca* 298 K.

PB was supplied by Polymer Standards Service, Mainz, and was composed of poly(1,4-butadiene) with a nominal average molecular weight of *ca* 100 000 g mol^{-1}, with minimal dispersity. Its glass transition temperature was around 170 K. The sample was transparent and extremely viscous at room temperature. It was always stored at a temperature of *ca* 276 K; when measurements had to be performed days apart, fresh samples were always used. At relatively high temperatures, extremely sharp liquid-like line-shapes were observed, corresponding to the long decay times of the free induction decay (FID) shown below. All this guarantees that any crystalline fraction, if present at all, can only appear in traces.

Methods

AFM force relaxation experiments were performed with a Bioscope microscope (Bruker Instruments) coupled to a Nanoscope IIIA controller. The temperature was controlled with a heat bath coupled to the sample support and it was continuously monitored with a digital thermometer equipped with a small K-thermocouple probe. Relaxation curves were obtained by applying a fast ramp

to the *z*-movement of the piezo-element (10 μm s^{-1}) to increase the force from zero to a set-point value (in the μN range); the movement of the piezo-element was then stopped (force raising time *ca* 30 ms). The relaxation of the force with time, as measured by the cantilever deflection, was then acquired by a digital oscilloscope. The relaxation step was not under a feedback control of the *z*-piezo movements. Accordingly, during the relaxation creep, even if the voltage applied to the piezo was constant, movements of the piezo in the vertical direction could be present. This behaviour was verified by performing relaxation tests on rigid surfaces (compared to the cantilever spring constant) such as mica or silicon oxide. We verified that the creep movement of the piezo was very small with respect to the overall sample deformation (less than 5%). Nevertheless, the creep movements measured on rigid samples in each experimental condition were subtracted from the force relaxation curves obtained. The cantilever used for relaxation experiments had a spring constant of 40 N m^{-1} (measured by the thermal method) and the tip apex (silicon) was modified by focused ion beam in order to obtain an almost spherical interacting region with a curvature radius of 2/3 μm. This tip assured stability during the measurements, a well-defined interacting geometry with the sample and an averaged interaction area large enough to avoid plastic deformation. All the reported measurements were obtained with the sample immersed in distilled water to avoid adhesion between the tip and the sample. The absence of adhesion was verified by AFM force curves.

The NMR experiments were carried out using a TecMag Apollo Double Resonance Spectrometer in the working range 5–450 MHz and a minimum digitization time resolution of 300 ns; a Bruker BM-10 variable field electromagnet was used. The measurement chamber was an Oxford CF1200 cryostat operating in the temperature range between 4 and 370 K. Systematic measurements were performed at three different values of the static magnetic field, respectively around 0.5 T, 1 T and 1.5 T. The intensity of the RF pulse used was 30 G ($\pi/2$ pulse duration 2 μs). Since the deadtime of the receiver is almost 5 μs, simple acquisition of the FID can fail when the decay of the signal is very fast and a significant part of it is lost. To avoid this problem, the FID signal was refocused using the magic sandwich echo (MSE) sequence.[10] The sequence used was the 'non-ideal' version with a train of $\pi/2$ pulses replacing the long bursts described by Rhim *et al.*,[10] with the aim of avoiding problems due to instrumental phase switching times between different pulses. From a mathematical point of view this sequence is substantially equivalent to the original one. A phase switching time of 3 μs was used (doubled during the groups of four pulses along the *x* axis constituting the core of the sequence), and the total length of the MSE sequence was 96 μs.

STRESS RELAXATION ANALYSIS

In this section, the analysis of a stress relaxation experiment on a sample of PnBMA is illustrated. This material was chosen because it is amorphous and its glass transition is at $T_g \approx 298$ K, so that a stress relaxation experiment by AFM can be performed near ambient temperature. Moreover, Donth's method has already been used to estimate the characteristic length of this material at T_g, yielding a reference value of $\xi \approx 1.0/1.3$ nm.[11]

Figure 1 shows the force relaxation curves at three representative temperatures. The curves have been aligned to the same initial force value (about 2.3 μN). All of them, as well as the others,

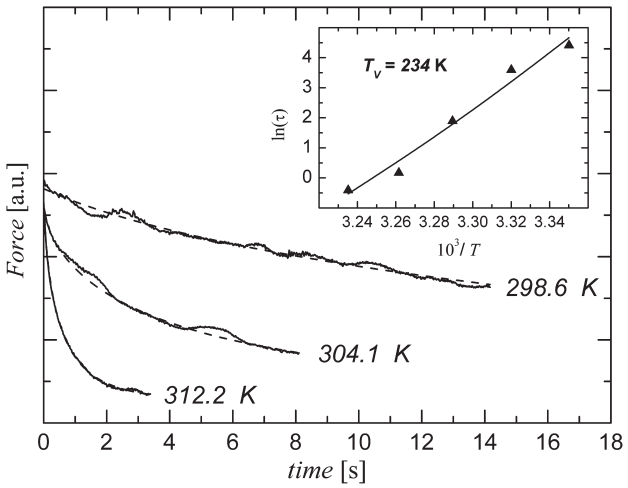

Figure 1. Force relaxation curves of PnBMA at three selected temperatures and the corresponding fittings (dashed lines) with a stretched exponential (Eqn (9)). The starting force value for relaxation is around 2.3 nN. The inset is a VFT plot of the average relaxation time τ, from which the Vogel temperature T_V can be estimated.

have been fitted with a stretched exponential function (the Kolrausch – Williams – Watts relaxation function):

$$\varphi_{KWW}(t) \propto e^{-\left(\frac{t}{\tau_{KWW}}\right)^{\beta}} \tag{9}$$

where β is the stretching exponent (related to the width of the frequency profile of the relaxation) and τ_{KWW} is a characteristic decay parameter from which the average relaxation time τ can be calculated:

$$\tau = \frac{\tau_{KWW}}{\beta}\Gamma\left(\beta^{-1}\right) \tag{10}$$

The temperature dependence of the latter quantity, reported in the inset of Fig. 1, has been fitted with a Vogel – Fulker – Tammann (VFT) function:

$$\tau = \tau_{\infty} e^{\frac{A T_V}{T - T_V}} \tag{11}$$

where τ_{∞} has been set to a value of 10^{-14} s in accordance with a wealth of relaxation data (see reference 12 and references therein), A is the fragility strength parameter and T_V is the Vogel temperature. In order to estimate the configurational entropy s_c, the T_V value for T_K in Eqn (7) suffices, so just the Vogel temperature will be considered throughout.

The fitting procedure yielded $T_V \approx 234$ K. The step of the specific heat Δc_p at T_g was estimated from the calorimetric data of Kahle *et al.*[11] and its ratio with the gas constant R is $\Delta c_p/R \approx 3.33$.

The stretching exponent β was found to decrease on approaching T_g, consistent with an increasing effect of the dynamic heterogeneity as cooperativity increased.

In order to estimate the parameters relevant to the evaluation of the CRR size, the relaxation function must be fitted with the following one, derived in the framework of the statistical mechanical model outlined above:[9]

$$\varphi(t) = \int_0^{\infty} d\zeta\, p(\zeta)\, e^{-t/\tau(\zeta)} \tag{12}$$

where

$$\tau(\zeta) \equiv \tau^* e^{z\,\Delta\mu(\zeta)/k_B T} \tag{13}$$

is the *actual* relaxation time of the z monomers in a configuration characterized by a barrier ζ and τ^* is a characteristic time scale of the attempts for crossing this barrier.

The analysis of the relaxation curve at $T \approx 298.6$ K, i.e. the closest one to T_g, yields $z = 2.8$, $\overline{\zeta} = 48.7$ kJ mol^{-1} and $\kappa = 0.5$, so that $N_\alpha \approx 43$ according to Eqn (8). Since the density of PnBMA is $\rho \approx 1.07$ g cm^{-3}, we find $\sqrt[3]{(N_\alpha M \rho N_A)} \approx 1.3$ nm, where M is the molecular weight of a monomeric unit and N_A is the Avogadro number. This result is in good agreement with the estimates of Donth[3], although it has been derived in a completely different way.

The amplitude of the CRR temperature fluctuation associated with the rearrangement can be estimated from the relation $\overline{\delta S \delta T} = k_B T$ [13]: by roughly assuming $\overline{\delta S \delta T} \approx \overline{\delta S} \cdot \overline{\delta T}$ we find in this case $\delta T \approx 8.5$ K. More refined estimates of this quantity can be done, providing a value $\delta T \approx 5.1$ K which is much closer to the literature data (i.e. $\delta T \approx 5.5/6.5$ K on cooling, $\delta T \approx 5.5/7.5$ K on heating in Donth[3]). The details, however, are not central to the present contribution and are deferred to a forthcoming paper (Pieruccini M and Alessandrini A, unpublished).

^{1}H NMR ANALYSIS

Isothermal patterns obtained by mechanical or broadband dielectric spectroscopy can be conveniently analysed in terms of Havriliak – Negami (HN) distributions in order to characterize the segmental relaxation properly. The present section illustrates the trackway through which this aim can be accomplished also by means of a suitable analysis of ^{1}H NMR data.

Theoretical background

We consider systems whose evolution, in the presence of a strong static magnetic field $\boldsymbol{B}_0$, is determined by a Hamiltonian where the spin pair interaction dominates, i.e.

$$H_{dip} = bP_2\left(\vec{I}\,\vec{J} - 3I_zJ_z\right) \tag{14}$$

where $\vec{I}$ and $\vec{J}$ are two $^1/_2$-spin operators associated with a pair of protons a distance d apart and $P_2 \equiv (3\cos^2\alpha - 1)/2$ is the second Legendre polynomial, with α the angle between the ideal segment joining the two protons and the direction of $\boldsymbol{B}_0$; b is related to the distance d and to the gyromagnetic ratio γ by

$$b = \frac{3\gamma^2\hbar}{4d^3}\frac{\mu_0}{4\pi} \tag{15}$$

The signal collected in a direction perpendicular to $\boldsymbol{B}_0$ after a $\pi/2$ pulse (i.e. the FID, or transverse relaxation function) carries information on the motion of the ensemble of spin pairs and, in particular, on the statistical evolution of the angle α of each pair, given the interaction Hamiltonian of Eqn (14). Due to the deadtime of the receiver, the FID signal has to be refocused for an analysis. This is achieved with an MSE pulse sequence, after which an FID with the *same shape* as the original one refocuses (see for example reference 14 and references therein). Due to molecular motions, however, the amplitude of the refocused FID may be lower than the original;[15] this circumstance will be central for the analysis below.

The transverse relaxation function may be expressed by the functional integral

$$\overline{G}(t) \equiv \Re \int \delta\psi(\tau)\, p[\psi(\tau)]\, e^{i\int_0^t d\tau\, bP_2[\alpha(\tau)]} \tag{16}$$

where $p[\psi(\tau)]$ is the probability associated with an angular trajectory of a spin pair during the time τ ($\psi \equiv (\alpha, \varphi)$, with φ the azimuthal angle in a plane perpendicular to $\boldsymbol{B}_0$). Statistically independent motions affecting the orientation dynamics can be introduced by simple superposition, given the linearity in $p(\psi)$. This is particularly useful when dealing with broad relaxation rate distributions, such as in the α-process.

In order to treat the effect of motion on the FID in the case of polymers, reference is usually made to the chain-like structure of these molecules, and pre-averaging over both fast segmental and β motions is done (or assumed) on deriving suitable analytical expressions for the discussion of experimental data.[15–17] In the present case, pre-averaging from just β motion is assumed, and an expression recently derived for the FID will be used for data analysis.[18] This expression is appropriate for a system consisting of an ensemble of spin pairs undergoing rotational diffusion, different pairs being considered as not mutually interacting. Implementing this model for the data analysis of a polymeric system, where multiple spin interactions may be important, can lead to poor estimates of the diffusion coefficient worked out from direct FID fittings; however, as shown below, this approximation is found not to appear as relevant on fitting the refocusing efficiency η, i.e. the ratio of the FID echo amplitude to that of the original one.

Details on the derivation of the relaxation function can be found in Sturniolo and Pieruccini;[18] for the present purposes it suffices to report the final result:

$$\overline{G}_n \equiv \Re\left\{R_n^{-1}\sum_{k=1}^{n}\mathrm{res}\left[W,\omega_k\right]e^{-i\omega_k t}\right\} \tag{17}$$

where $R_n \equiv \sum_{k=1}^{n} res\left[W,\omega_k\right]$, with $W \equiv W(\omega, D, b)$ a function of the complex angular frequency ω, the rotational diffusion (real) coefficient D and the coupling constant b. This function can be represented as a continued fraction; n indicates the order of its rational approximation. The n residues of this truncated expansion are calculated in the respective poles ω_k. From the physical point of view, approximating to order n means that the evolution process of the whole system is described through a representative finite subset of n spin pairs; $\overline{G}_n$ coincides with the exact solution of the problem up to a certain limiting time t_n; on increasing n, t_n increases. In the present conditions (see below), no more than seven poles were found to suffice for a satisfactory analysis.

Note that

$$\overline{G}_n(t_1+t_2) = \Re\left\{R_n^{-1}\sum_{k=1}^{n}\mathrm{res}\left[W,\omega_k\right]e^{-i\omega_k(t_1+t_2)}\right\} \tag{18}$$

Therefore, while the coefficients res$[W, \omega_k]$ describe the evolution of the representative subset starting from an initial condition ($t = 0$) where the angular distribution of the spin pair ensemble is a δ function, the coefficients res$[W, \omega_k]$ exp$(-i\omega_k t_1)$ describe the evolution for $t \geq t_1$ from an 'initial' condition (i.e. at $t = t_1$) where this angular distribution has already broadened to some extent.

MSE allows us to refocus an echo of a dipolar dephased FID with excellent fidelity even long after its decay (more than 100 μs). If the coupling strength in the system remains constant during the whole experiment, then the refocusing will be complete and the ratio η between the intensity of refocused FID to that of the original one is unity ($\eta = 1$). This condition may break down due to molecular motions, causing the decrease of the echo amplitude.

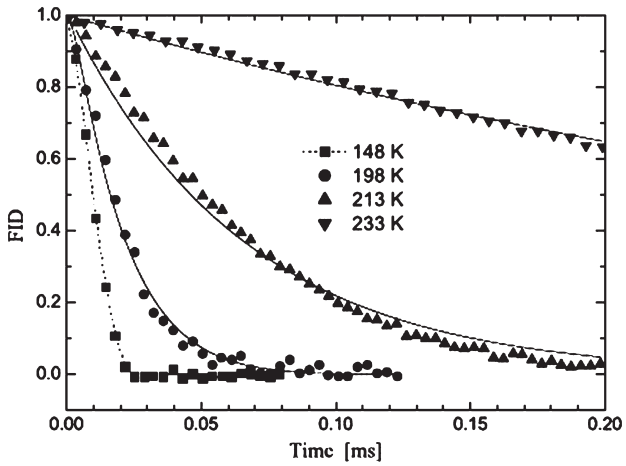

Figure 2. MSE refocused FIDs in PB at different temperatures in a static field corresponding to a Larmor frequency of 22 MHz (symbols) and their respective fittings according to Eqn (17) (solid lines) for $n = 20$. The dotted line for the $T = 148$ K FID is just a guide for the eye.

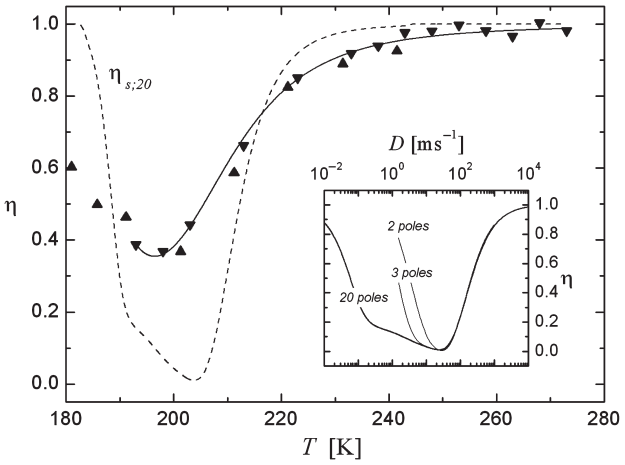

Figure 3. MSE efficiencies obtained in two sets of measurements at 22 MHz (up and down triangles). The dashed line corresponds to the single-*D* efficiency $\eta_{s;20}$ for $\tau = 16$ μs, $b = 300$ kHz and D calculated as explained in the text. The solid line is a fit to the data with a distribution of single-*D* efficiencies as expressed by Eqn (20). The inset shows the theoretical efficiency as a function of D for different numbers of poles and the same b.

As a function of the extent of molecular motions, η is close to 1 for frequencies that are either very low or very high compared to the order of magnitude of the dipolar coupling constant, being drastically reduced when the two frequencies are similar.[19]

An estimate of the MSE refocusing efficiency may be obtained following the evolution of the representative subset when a pulse sequence $\{\tau_+ \mid 4\tau_- \mid \tau_+\}$ is imposed, such that in the intermediate interval the Hamiltonian governing the evolution of the system is multiplied by a factor $-1/2$, providing an effective time reversal (with the exclusion of the diffusion process, of course).[10] After Eqn (18) and the related comments, in the case of a single-*D* diffusion process we find the following expression for the efficiency:

$$\eta_{s;n} = \Re\left\{ R_n^{-1} \sum_{k=1}^{n} \mathrm{res}\left[W, \omega_k\right]\ e^{-i\left(2\omega_k\big|_{\tau_+} - 4\omega_k^*\big|_{\tau_-}\right)\tau} \right\} \qquad (19)$$

(the subscript s standing for 'single-*D*') where the poles $\omega_k\big|_{\tau_+}$ and $\omega_k\big|_{\tau_-}$ are calculated with coupling constants b and $-b/2$ respectively. This expression will subsequently be used to fit the temperature profile of the MSE refocusing efficiency.

Experimental results

Figure 2 reports the FIDs collected for selected temperatures, together with their associated single-*D* fittings with $\overline{G}_{20}(t)$, i.e. obtained with $n = 20$ (the dotted line for the lowest T is just a guide for the eye). Following the prescriptions of Papon *et al.*,[15] the coupling constant has been estimated from the lowest temperature FID just above T_g (i.e. $T = 173$ K), yielding $b \approx 300$ kHz.

Figure 3 shows how the experimental values of the efficiency compare with a single-*D* theoretical efficiency derived for $n = 20$. In order to do this comparison, the $D(T)$ dependence was momentarily calculated from the relation $D = (6\tau_c)^{-1}$, with τ_c the relaxation time associated with the $\langle P_2 \rangle$ decay, i.e. $\langle P_2 \rangle \sim \exp(-t/\tau_c)$ (see for example Sturniolo and Pieruccini[18]) and from the assumption that τ_c follows the same VFT relation of the α-process observed by dielectric spectroscopy.[20] Below, the VFT parameters for $\tau_c(T)$ (or equivalently for $D(T)$) will be re-calculated from the fittings on η.

The matching with the efficiency dip is remarkable; however, it is evident that a distribution of D needs be considered for a good fit to the experimental data. In other words, the T dependence of η found experimentally carries information on the distribution of relaxation times in the system. In order to extract this information, the data are fitted with a superposition of single-*D* contributions, i.e.

$$\eta(T) = \int_{-\infty}^{+\infty} F_\alpha\left[D, D_c(T)\right]\ \eta_s(D)\ \mathrm{d}\ln D \qquad (20)$$

where, for convenience, F_α is chosen as the normalized distribution from which the HN function can be generated:

$$F_\alpha\left(D, D_c\right) = \frac{\left(\frac{D_c}{D}\right)^{ac} \sin(c\phi)}{\pi\left[1 + 2\left(\frac{D_c}{D}\right)^{a}\cos(\pi a) + \left(\frac{D_c}{D}\right)^{2a}\right]^{c/2}} \qquad (21)$$

with D_c the 'central' diffusion constant,

$$\phi = \arctan\left[\frac{\sin(\pi a)}{(D_c/D)^a + \cos(\pi a)}\right] + \pi\left\{1 - \Theta\left[\frac{\sin(\pi a)}{(D_c/D)^a + \cos(\pi a)}\right]\right\} \qquad (22)$$

and Θ is the Heaviside step function. If $\eta_s(D)$ is replaced with the function $[1 + i\omega/(6D)]^{-1}$ in Eqn (20), we find indeed the HN form of the relaxation profile, i.e. $\{1 + [i\omega/(6D_c)]^a\}^{-c}$ where a and c (both varying within the interval [0, 1]) are respectively the width and symmetry parameters of the frequency distribution.

The solid line in Fig. 3 is a fitting to the data with the efficiency expressed by Eqn (20) and $n = 7$ (using higher n values did not change the results significantly). A VFT dependence on T was assumed for D_c, with T_V and A free to adjust; on the other hand, consistently with the assumptions made in the previous section, a τ_∞ value of 10^{-14} s was imposed. The shape parameters of the HN distributions were also let free to adjust, yielding at the end $a \approx 0.55$ and $c \approx 0.45$. With regard to the VFT parameters, the values $A = 12.05$ and $T_V \approx 130$ K were found. The latter is in fairly

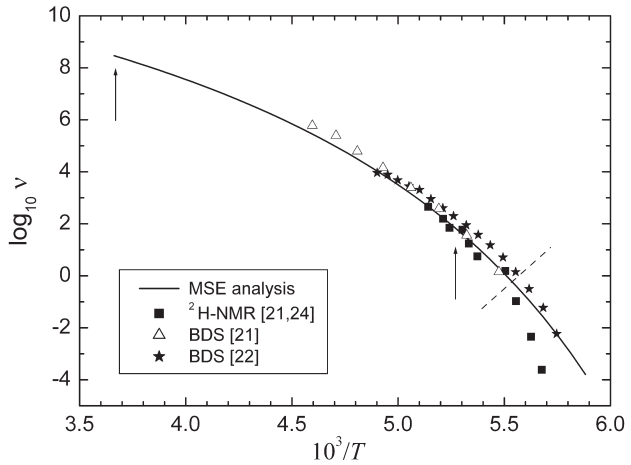

Figure 4. VFT plot of $\nu(T)$ as obtained from the analysis of the MSE refocusing efficiency and comparison with the corresponding behaviour resulting from the parameters provided by Deegan and Nagel.[20] The T dependences of the central relaxation frequencies of the literature are also reported for a comparison. The arrows indicate the T^{-1} bounds within which the ^{1}H NMR measurements were actually performed. Note that the extrapolation to lower temperatures still compares well with the BDS relaxation data of Arbe *et al.*[21] The dashed segment marks a lower T bound beyond which deviations from the ^{2}H NMR data of Deegan and Nagel[20] and Rössler *et al.*[23] start to be significant.

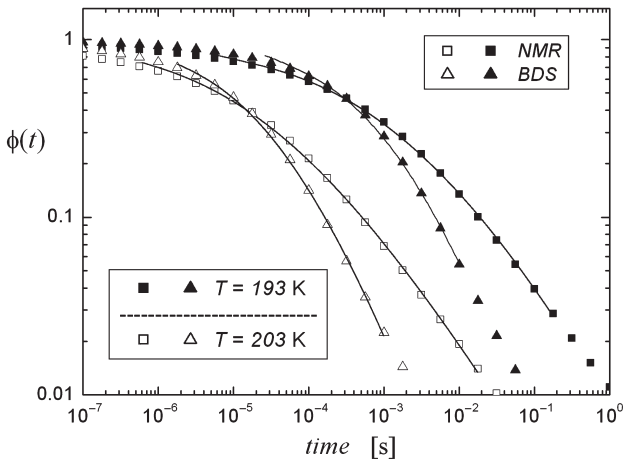

Figure 5. Relaxation functions associated with the HN parameters of the α-processes in PB, as observed by means of BDS[21] or deduced from the analysis of the MSE efficiency for two temperatures (symbols). The solid lines are best fits from which the parameters reported in Table 1 can be obtained.

good agreement with the viscosity data provided by Arbe *et al.*[21] concerning the T dependence of the central relaxation time.

Figure 4 reports the VFT behaviour of $\nu \equiv (2\pi\tau_c)^{-1}$ as derived from the MSE efficiency with the procedure described above (solid line). This dependence is compared with that obtained introducing in the VFT expression for τ the parameters provided by Deegan and Nagel[20] on the basis of BDS data (triangles). Although the two $\nu(T)$ curves are fairly close to each other, the associated parameters are different ($\tau_\infty \approx 7.6 \times 10^{-14}$ s, $A \approx 7.96$ and $T_V = 142$ K) because in the present case τ_∞ has been fixed. The value of 142 K seems to be rather larger than those which can be obtained by fitting the viscosity ($T_V = 122$ K) or other BDS data ($T_V = 130.6$ K) from Arbe *et al.*[21] under the same constraint of $\tau_\infty = 10^{-14}$ s (the latter are replotted as stars in Fig. 4 for convenience). Also, a value of $T_V = 128$ K has been reported by Frick and Richter.[22] Data on PB obtained by stimulated echo ^{2}H NMR are also reported for comparison.[23]

CRR size

As illustrated in the section Cooperative motion, the size of the large scale cooperativity regions can be estimated from the relaxation functions once T_K (which can be safely replaced by T_V since it only enters in the argument of the logarithm and the measurement temperature is high enough compared with T_V itself) and Δc_p are known. If Donth's approach is used instead, estimating the average CRR size requires a precise determination of the specific heats below and above T_g, which needs a careful calibration of the calorimeter (see for example Saiter *et al.*[24] and Schick[25]).

From the calorimetric data provided by Bähr *et al.*[26] we have $\Delta c_p \approx 0.52$ J g^{-1} K^{-1}; since the density of PB is *ca* 0.87 g cm^{-3}, its ratio with the gas constant is $\Delta c_p/R \approx 3.4$. On the other hand, a T_V value of 130 K results from the MSE efficiency fitting, while from the BDS data of Arbe *et al.*,[21] replotted in Fig. 4, we find the Vogel temperature reported above (i.e. 130.6 K).

Figure 5 shows the relaxation functions (and the corresponding fittings) extracted from BDS and NMR analyses at temperatures of 193 and 203 K. These values are the extremes of the T interval within which both NMR and BDS data from Arbe *et al.*[21] are available. The best fitting parameters are reported in Table 1; the results show that the two techniques used to probe segmental relaxation, although rather different, provide similar estimates for the cooperativities. The only discrepancy seems to arise from the difference in the HN width parameter. The value of $a = 0.72$ ascribed to the BDS relaxation distribution, however, was just inferred in Arbe *et al.*[21] and not directly derived from the loss profile analysis. Overall, the BDS relaxation functions turn out to decay more rapidly than those obtained from the NMR experiments; this is why a comparatively lower number of rearranging units is found from dielectric analysis. Concerning the actual number of monomers involved in the rearrangement, it is important to note that each technique provides a CRR size which increases on lowering T; this behaviour is expected in general (see also Hamonic *et al.*[4], Dalle-Ferrier *et al.*[27] and Capaccioli *et al.*[28]) and has recently been reported by Chua *et al.*[29] where nice calorimetric analyses are performed on amorphous poly(styrene) and poly(methyl methacrylate). Note that in the spresent case the temperature is not very close to T_g so the CRR sizes are relatively small. As illustrated above, the comparatively narrower frequency distribution derived from the BDS data of Arbe *et al.*[21] yields N_α values which are correspondingly smaller than those obtained by NMR; this incidentally provides the same CRR size from BDS at $T = 193$ K and from ^{1}H NMR at 203 K.

CONCLUDING REMARKS

The distinction of the two length scales involved in the cooperative rearrangement process is essential in the analysis of the relaxation data and in the final estimate of the average CRR size. Consider for instance the stress relaxation experiment illustrated above. The decrease in time of the force probed by AFM is ultimately due to the material yield triggered by local cooperative configurational rearrangements. The analysis of the pattern works out some of its characteristic features, namely those related to just the small scale rearrangement. Only afterwards are these quantities used to calculate the CRR size, i.e. the large scale rearrangement length.

In Donth's approach, instead, scanning temperature relaxation measurements (e.g. calorimetric or dielectric[4]) are needed to

Table 1. Temperature T (the measurement technique to which the values of the line refer is indicated in parentheses), central relaxation time τ_0 (BDS data are from Arbe *et al.*[21]), fitting parameters λ, z, τ^* (and n), lower limit of the fitting interval t_{min}, and resulting values for average energy threshold $\langle\xi\rangle \equiv \left[\int_0^\infty d\zeta\, p\right]^{-1} \int_0^\infty d\zeta\, \zeta\, p$, rearrangement chemical potential $\overline{\Delta\mu}$ and its dispersion around the mean $\delta[\Delta\mu]$, fraction κ of CRRs inducing diffusive configurational changes and total number of rearranging monomers N_α, for the α-relaxation process of PB. The HN shape parameters a and c are 0.55 and 0.45 for the NMR measurements and 0.72 and 0.50 respectively for BDS (following the indications of Arbe *et al.*[21])

T (K)	τ_0 (s)	n	λ	z	τ^* (s)	t_{min} (s)	$\langle\xi\rangle$ (kJ mol^{-1})	$\overline{\Delta\mu}$ (kJ mol^{-1})	$\delta[\Delta\mu]$ (kJ mol^{-1})	κ	N_α
193 (NMR)	4×10^{-3}	14	14.4	5.5	3×10^{-6}	5×10^{-6}	23	1.42	0.92	0.2	≈14
203 (NMR)	1.1×10^{-4}	8	6.7	3.7	2×10^{-7}	6×10^{-7}	15.9	2	1.38	0.31	≈9
193 (BDS)	1.8×10^{-3}	13	13	3.2	2×10^{-5}	2.6×10^{-5}	21.7	1.5	1	0.22	≈9
203 (BDS)	6×10^{-5}	10	8.5	2.7	6×10^{-7}	2×10^{-6}	19.2	1.96	1.25	0.27	≈7

estimate the temperature fluctuations characterizing the CRRs. Their amplitude is indeed related to the CRR size by $\overline{\delta T^2} N_{ff} \approx k_B T^2 \Delta\left(1/c_p\right)$,[3] where Δ indicates the difference between the values above and below the glass transition. In some sense, this method probes the CRR size directly, while in the above procedure the latter is *calculated* from the small scale readjustment features. Notwithstanding these significant differences, the two methods provide mutually consistent results.

The approach proposed in the present paper has the advantage of being open, at least in principle, to the treatment of confinement problems by appropriately writing down the expression of the configurational entropy. On the other hand, there are still aspects of the theory which need to be developed. In particular, working out a suitable expression for τ^* in order not to let it remain just a fitting parameter would represent a significant improvement, and in this direction work is presently being undertaken.

As expected also in other frameworks,[2,4,27,28] the CRR size is found to increase on cooling towards T_g. This has been shown explicitly for PB in the present contribution and it has also been verified both for PnBMA and for semicrystalline PET.[8]

To conclude, we would like to draw attention to the method we used to extract the relevant information about the distribution of segmental relaxation times in PB. The derivation of the analytical expression for the FID refocusing efficiency requires methods of complex analysis, but as a final result one has the advantage that this information can be worked out from the experiment without, for example, the need to use deuterated samples (cf. the ^{2}H NMR experimental data of Fig. 4). Comparisons with the results obtained with other techniques (cf. Fig. 4) give a feeling about the reliability of our procedure, at least for PB. Of course, further checks on different systems are under way.

REFERENCES

1 Adam G and Gibbs JH, *J Chem Phys* **43**:139–146 (1965).
2 Donth E, *The Glass Transition: Relaxation Dynamics in Liquids and Disordered Materials*, *Springer Series in Materials Science*, vol. 48, Springer-Verlag, Berlin/Heidelberg (2001).
3 Donth E, *J Polym Sci B Polym Phys* **34**:2881–2892 (1996).
4 Hamonic F, Prevosto D, Dargent E and Saiter A, *Polymer* **55**:2882–2889 (2014).
5 Dokukin ME and Sokolov I, *Langmuir* **28**:16060–16071 (2012).
6 Martínez-Tong DE, Najar AS, Soccio M, Nogales A, Bitinis N, López-Manchado MA *et al.*, *Compos Sci Technol* **104**:34–39 (2014).
7 Braunsmanna C, Proksch R, Revenko I and Schäffer TE, *Polymer* **55**: 219–225 (2014).
8 Pieruccini M, arXiv [Cond-mat.soft]: 1410.7562v1.
9 Pieruccini M and Ezquerra TA, *Eur Phys J E* **29**:163–171 (2009).
10 Rhim W-K, Pines A and Waugh JS, *Phys Rev B* **3**:684–696 (1971).
11 Kahle S, Korus J, Hempel E, Unger R, Höring S, Schröter K *et al.*, *Macromolecules* **30**:7214–7223 (1997).
12 Linares A, Nogales A, Sanz A, Ezquerra TA and Pieruccini M, *Phys Rev E* **82**: 031802-1/11 (2010).
13 Donth E, *J Non-Cryst Solids* **307–310**, 364–375 (2002).
14 Sturniolo S, Pieruccini M, Corti M and Rigamonti A, *Solid State NMR* **51–52**:16–24 (2013).
15 Papon A, Saalwächter K, Schäler K, Guy L, Lequeux F and Montes H, *Macromolecules* **44**:913–922 (2011).
16 Fechete R, Demco D and Blümich B, *J Chem Phys* **118**:2411–2421 (2003).
17 Brereton M, *J Chem Phys* **94**:2136–2142 (1991).
18 Sturniolo S and Pieruccini M, *J Mag Res* **223**:138–147 (2012).
19 Sturniolo S and Saalwächter K, *Chem Phys Lett* **516**:106–110 (2011).
20 Deegan RD and Nagel SR, *Phys Rev B* **52**:5653–5656 (1995).
21 Arbe A, Richter D, Colmenero J and Farago B, *Phys Rev E* **54**:3853–3869 (1996).
22 Frick B and Richter D, *Science* **267**:1939–1945 (1995).
23 Rössler E, Warschewske U, Eiermann P, Sokolov AP and Quitmann D, *J Non-Cryst Solids* **172–174**:113–125 (1994).
24 Saiter A, Prevosto D, Passaglia E, Couderc H, Delbreilh L and Saiter JM, *Phys Rev E* **88**:042605-1/7 (2013).
25 Schick C Temperature modulated differential scanning calorimetry (TMDSC) - basics and application to polymers, in *Handbook of Thermal Analysis and Calorimetry*, vol. **3**, ed. by Cheng S. Elsevier, New York, 713 pp. (2002).
26 Bähr M, Schreier F, Wosnitza J, Löhneysen HV, Zhu C, Qin X *et al.*, *Europhys Lett* **22**:443–448 (1993).
27 Dalle-Ferrier C, Thibierge C, Alba-Simionesco C, Berthier L, Biroli G, Bouchaud J-P *et al.*, *Phys Rev E* **76**:041510-1/15 (2007).
28 Capaccioli S, Ruocco G and Zamponi F, *J Phys Chem B* **112**: 10652–10658 (2008).
29 Chua YZ, Schultz G, Shoifet E, Huth H, Zorn R, Schmelzer JWP *et al.*, *Coll Polym Sci* **292**:1893–1904 (2014).

